creative commons
COMMONS DEED

저작자표시-비영리-변경금지 2.0 대한민국

이용자는 아래의 조건을 따르는 경우에 한하여 자유롭게

- 이 저작물을 복제, 배포, 전송, 전시, 공연 및 방송할 수 있습니다.

다음과 같은 조건을 따라야 합니다:

저작자표시. 귀하는 원저작자를 표시하여야 합니다.

비영리. 귀하는 이 저작물을 영리 목적으로 이용할 수 없습니다.

변경금지. 귀하는 이 저작물을 개작, 변형 또는 가공할 수 없습니다.

- 귀하는, 이 저작물의 재이용이나 배포의 경우, 이 저작물에 적용된 이용허락조건을 명확하게 나타내어야 합니다.
- 저작권자로부터 별도의 허가를 받으면 이러한 조건들은 적용되지 않습니다.

저작권법에 따른 이용자의 권리는 위의 내용에 의하여 영향을 받지 않습니다.

이것은 이용허락규약(Legal Code)을 이해하기 쉽게 요약한 것입니다.

Disclaimer

dCollection

공학석사학위논문

Dependence of Bias Stress on Hydrophobicity of Gate Insulator in Organic Thin-Film Transistors

유기 박막 트랜지스터에서의 게이트 절연막의 소수성에 대한 바이어스 스트레스 의존성 연구

2016 년 8 월

서울대학교 대학원

전기정보공학부

노 완 우

Dependence of Bias Stress on Hydrophobicity of Gate Insulator in Organic Thin-Film Transistors

유기 박막 트랜지스터에서의 게이트 절연막의 소수성에 대한 바이어스 스트레스 의존성 연구

지도교수 이 신 두

이 논문을 공학 석사 학위 논문으로 제출함

2016 년 5 월

서울대학교 대학원

전기정보공학부

노 완 우

노완우의 공학 석사 학위 논문을 인준함

2016 년 6 월

위 원 장 이 창 희 (인)

부위원장 이 신 두 (인)

위 원 홍 용 택 (인)

Abstract

Organic thin-film transistors (OTFTs) have been paid great attention due to their potential for low-cost, large-area, and flexible electronics. Recently, the electrical performances such as field-effect mobility have come close to or even exceeded those of typical amorphous silicon transistors. Nonetheless, the operational instability of OTFT devices has been considered as a serious obstacle in use for practical applications. Among various factors, the surface properties of a gate insulator which determine charge trapping at the interface between an active layer and a gate insulator strongly influence the stability. In particular, the hydrophobicity of a gate insulator has been thought to play an important role when it comes to moisture in the atmosphere since it has been reported that the water molecules act as main trap sites and cause the instability of the OTFT. However, the effect of the hydrophobicity on the stability has not been elaborated so far because replacement of material for a gate insulator to modify the hydrophobicity is inevitably accompanied by the change in the other surface properties as well.

In this work, we report the effect of the hydrophobicity of a gate insulator on the stability of the OTFT, in particular, the shift of the threshold voltage by the gate bias stress. For the investigation of the effect, OTFTs comprised of the same materials but having different hydrophobicity for a gate insulator were fabricated in a bottom-gate top-contact configuration using a solution-processed TIPS-pentacene as an active layer. Here, a hydrophobic fluoropolymer, CYTOP, was used for a gate insulator since the hydrophobicity can be modified without changing other surface properties using the aluminum-assisted method based on the reorientation of end functionalities described elsewhere. Depending on the hydrophobicity of the gate insulator, the value of threshold voltage shift after applying the gate bias stress of −20 V for 1000 s was found to significantly decrease from −13.42 V to −2.56 V on average. It was attributed to the suppression of the trap formation owing to water repellency as well as non-polar end functionalities of the hydrophobic interface. Our studies would help to understand the effect of the hydrophobicity on the stability toward highly reliable OTFT devices for a variety of applications including flexible electronics.

Key Word: Solution-processed organic thin-film transistors, Gate bias stress, Hydrophobicity, TIPS-pentacene, CYTOP

Student ID: 2014-22555

TABLE OF CONTENTS

LIST OF FIGURES

1. Introduction

1.1. Stability Issue of Organic Thin-Film Transistors (OTFTs)

In recent years, organic thin-film transistors (OTFTs) have been extensively studied owing to their potential for low-cost, large-area, and flexible electronics [1-2]. In particular, for small molecule organic semiconductors (OSCs), the values of the field-effect mobility have been increased to exceed that of typical amorphous silicon as shown in the Fig. 1.1 [3-4]. Nevertheless, the operational instability of the OTFT such as the gate bias stress effect has been considered as a serious obstacle before commercialization [5-7].

The electrical instability is mainly due to charge trapping and releasing in a variety of regions in the OTFT [5-13]. It could be a serious problem for operating devices and circuits since it may lead increase or reduction of current level at a given voltage. Therefore, there have been numerous attempts to understand the physical mechanism of the instabilities during OTFT operation.

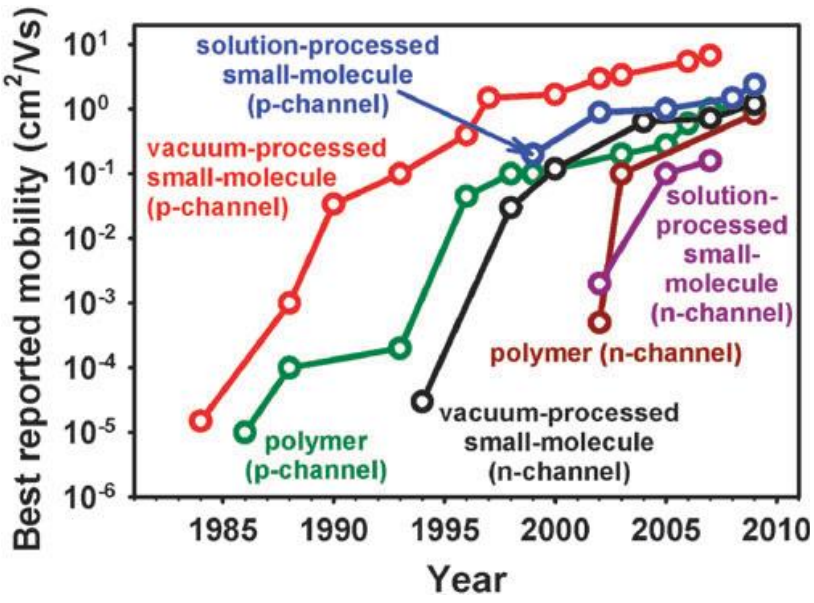

Fig. 1.1. Development of carrier mobility in OTFT [14].

1.2. Effect of Hydrophobicity on Stability of OTFTs

From the viewpoint of the charge traps, the surface properties of a gate insulator, which is interfaced with an active layer, such as the surface roughness [9], the density of hydroxyl groups [10], and the hydrophobicity [11] significantly influence the instability of the OTFT. Among them, the hydrophobicity of the gate insulator plays an important role in the formation of charge traps under ambient environment

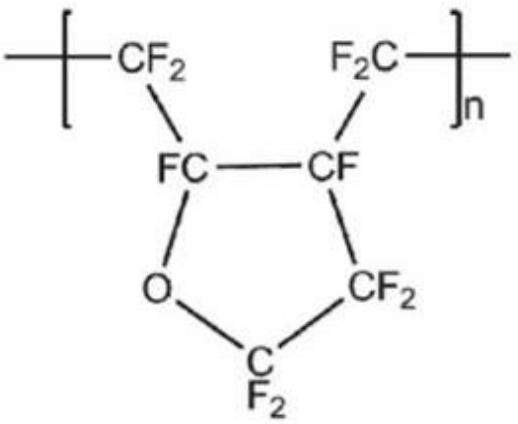

Fig. 1.2. The chemical structure of the CYTOP.

of the moisture because it has been reported that water molecules, diffused into the interface, act as trap sites that primarily cause the instability of the OTFT [12-13]. In other words, a hydrophobic gate insulator may resist water molecules and enhance stability of the OTFT. For example, poly(1,1,2,4,4,5,5,6,7,7-decafluoro-3-oxa-1,6-heptadiene) (CYTOP) has been used as a gate insulator or a passivation layer for high operational stability against the gate bias stress due to its hydroxyl-free and hydrophobic surface properties [15-17]. The chemical structure of the CYTOP is illustrated in Fig.1.2. However, due to the poor wettability of an organic solvent

dissolving the small molecule OSC on it, the use of the intrinsic CYTOP as a hydrophobic gate insulator in a bottom-gate configuration, which has several advantages [18], is quite limited. In addition, since it is difficult to separate the sole effect of hydrophobicity on the stability of OTFTs from the effect of other surface properties, the direct relationship between the surface properties and stability of OTFTs has not been examined in the earlier studies accompanying the material change.

In this work, we investigated how the hydrophobicity of a gate insulator influences the bias stress in OTFTs. In the bottom-gate configuration of the OTFT with a solution-processed OSC layer, the hydrophobicity of the insulator layer of the CYTOP, prepared through a sequential process of the deposition and removal of an aluminum layer on it, was thoroughly varied with changing the post-annealing temperature. The detailed procedure and mechanism of aluminum-assisted surface hydrophobicity modification method will be discussed in the subsequent chapters. Fig. 1.3 schematically illustrates a cross-sectional view of our OTFT device structure in a bottom-gate top-contact configuration.

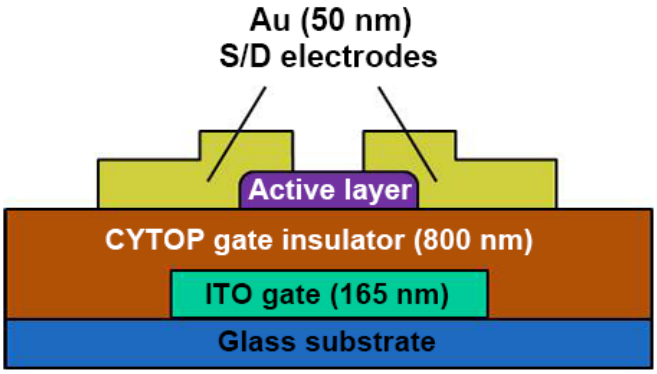

Fig. 1.3. A schematic diagram of the OTFT we fabricated.

1.3. Outline of Thesis

This thesis consists of five chapters from **Introduction** to **Conclusion**. In **Chapter 1,** the general overview for the operational instability issue of the OTFT is introduced. The brief description of this research and what will be discussed are also introduced. Also, why there have been many attempts to understand this issue is discussed in this chapter. **Chapter 2** provides the theoretical background for understanding the basic principles and charge trapping mechanism of the OTFT. A novel method of controlling surface hydrophobicity using aluminum-assisted

method will be introduced. **Chapter 3** presents the experimental procedures of this research are described. The method of analysis and whole process of fabricating our device using aluminum-assisted method are covered. In **Chapter 4**, the results of experiments are presented and discussed. Finally, in **Chapter 5**, some concluding remarks are made.

2. Theoretical Background

2.1. Basic Principles of OTFTs

An OTFT is a field-effect transistor whose active layer is comprised of organic semiconductors and it is also known as OFET (Organic Field-Effect Transistors). Similar to a common silicon-based metal-oxide-semiconductor field-effect transistor (MOSFET), the basic operating principle of OTFT is to control the flow of charge carrier in the channel region between the source and drain electrode by applying voltage to the gate electrode. However, the channel formation is quite different from MOSFET in that the channel of an OTFT is formed in the accumulation region whereas that of MOSFET is formed in the inversion of the charge. According to the most prevailed theory, the charge carrier transport in organic semiconductor is shown as a mechanism of hopping transport by thermal activation, while band transport occurs in the silicon-based MOSFET.

2.1.1. Parameters and Characterization

Fundamentally, an OTFT operates like a capacitor that produces the electric field in the gate dielectric at positive or negative gate voltage for n-type or p-type organic semiconductor materials. The structure and operation of an OTFT is schematically depicted in Fig. 2.1. On applying a bias between the gate and source (V_{GS}), a sheet of mobile charge carriers is accumulated, which is called a channel, near the interface of semiconductor and insulator that allows the flow of current through the active

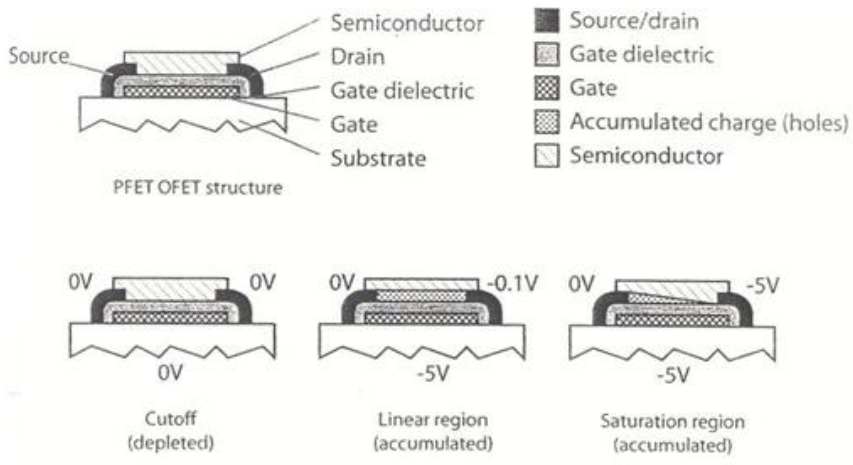

Fig. 2.1. A schematic showing the structure and operation of an OTFT [19].

layer on applying a suitable drain to source potential (V_{DS}). A minimum value of gate voltage required for formation of charge carrier channel at the interface is known as the threshold voltage (V_{TH}). The threshold voltage plays an important role in operating OTFT in that it determines the switching behavior of a device. An OTFT device of lower threshold voltage has an advantage of low power consumption.

As long as the drain voltage remains lower than the overdrive voltage ($V_{DS} < V_{GS}-V_{TH}$), the drain current builds up linearly due to the presence of carriers all along the channel. Furthermore, a magnitude of the drain voltage close to $V_{GS}-V_{TH}$, results in a non-linear increase in the current. Finally, at $V_{DS} = V_{GS}-V_{TH}$, the current saturates due to pinching-off of the channel and further increase in V_{DS} does not contribute in enhancing the magnitude of the current. At the saturation region, the current between the drain and source electrodes is expressed as

$$I_{DS} = \frac{W}{2L} C_i \mu (V_{GS} - V_{TH})^2$$

where W is the channel width, L is the channel length, C_i represents the gate dielectric capacitance per unit area, and μ is the mobility of the device which

represents the average charge carrier drift per unit electrical field.

For extracting electrical parameters such as μ and V_{TH}, it is necessary to plot I_{DS} as a function of V_{GS}. The relationship between I_{DS} and V_{GS} is called transfer characteristics. Though there have been many approaches to extract these parameters, the extrapolation method in the saturation region are commonly used. The method is illustrated in Fig. 2.2. The value of V_{TH} and μ can be extracted from the x-intercept and the slope of the linear part of $I_{DS}^{1/2}$ - V_{GS} plot fitting the data to the equation of drain current.

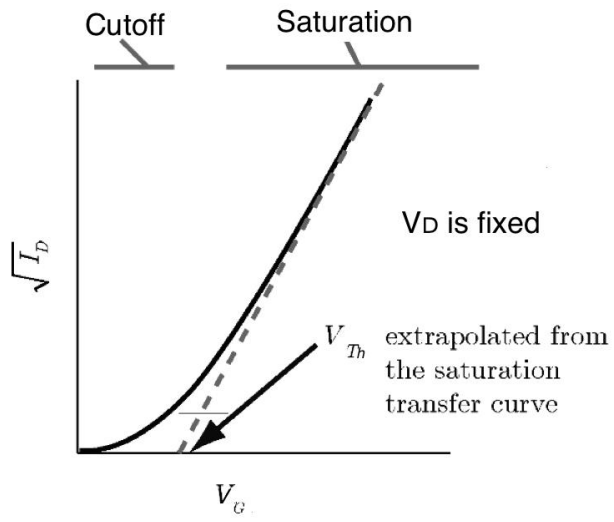

Fig. 2.2. Extraction of threshold voltage from $I_{DS}^{1/2}$ - V_{GS} plot by extrapolation method in saturation region [19].

2.1.2. Device Structure and Configuration

The OTFTs have been fabricated with various device geometries. Depending on the arrangement of the gate electrode, top-gate (TG) and bottom-gate (BG) structure are distinguished. Also, for the position of a source and drain contact with respect to the organic semiconductor layer, the structure of OTFT named as top-contact (TC) and bottom-contact (BC) structures. Thus, there are four different structures relying on

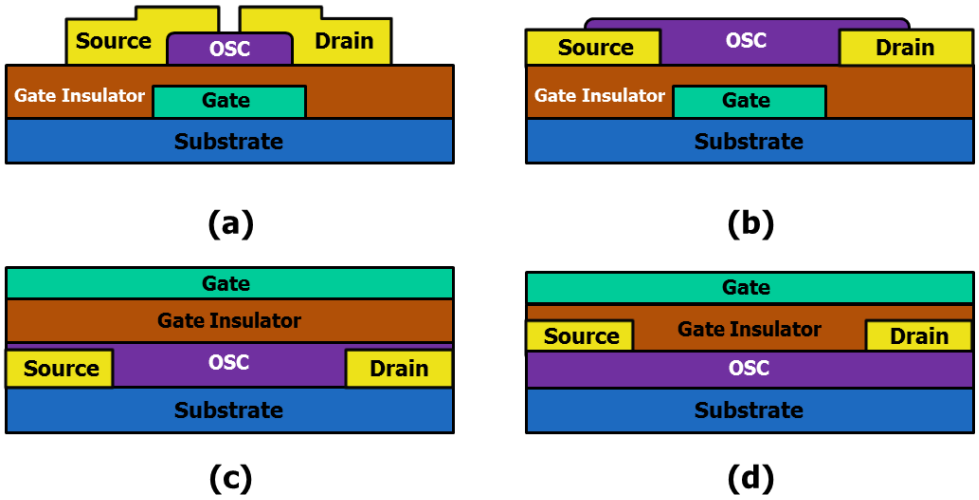

Fig. 2.3. The configurations of (a) BGTC, (b) BGBC, (c) TGBC, and (d) TGTC.

the position of each layer and these are depicted as Fig .2.3. Each configuration has its own features. First, BG structure is commonly superior to TG in its electrical performance due to the possible deterioration of organic semiconductor layer during thermal deposition of gate electrode [14]. Also, it is easier to deposit an OSC layer on gate insulator material than to deposit reversely. Instead, TG configuration could provide the encapsulation of OSC layer and thus enhances stability of the device if orthogonality issue is solved [17].

The TC configuration exhibits a better performance compared to BC device

due to its lower contact resistance and large injection area [20]. Additionally, TC OTFTs show less morphological disorder in the active layer than BC OTFTs. However, for BC OTFTs, it is possible to apply lithographic patterning method, leading to achieving high resolution of patterning in channel area. Moreover, BC configuration has better compatibility than TC configuration [21].

2.2. Gate Bias Stress Effect Induced by Trap Formation

Operational instability of OTFT can be shown as a variety of phenomena such as the decrease in field-effect mobility [22-23], hysteresis [24], and threshold voltage shift [14]. First, the cause of decrease in field-effect mobility is mainly known to the degradation or oxidation of organic semiconductor. Many studies have shown that the current hysteresis is induced by short-term trapping and release of charge carriers while the threshold voltage shift is due to long-term trapping and release of charge carrier. In this work, we will discuss about the threshold voltage shift since the analysis is most convenient as well as the effect on device operation is highly

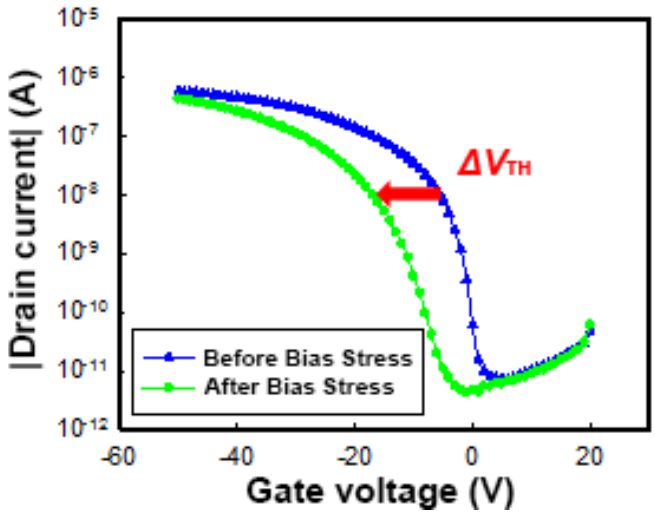

Fig. 2.4. Threshold voltage shift showed in the transfer characteristics.

important. For instance, the display panel may not turn on or off if the threshold voltage has largely shifted. Threshold voltage shift normally occurs when the gate bias stress is applied to OTFT and this is called gate bias stress effect. Fig. 2.4 shows how threshold voltage shift appears in the I-V transfer characteristics curves.

On the other hand, charge trapping and release in the OTFT could occur in a range of regions but mainly in the three vulnerable parts, which are the bulk of the semiconductor, the bulk of the gate insulator, or in the interface between the semiconductor and gate insulator [5]. Fig. 2.5 shows how the charge traps are

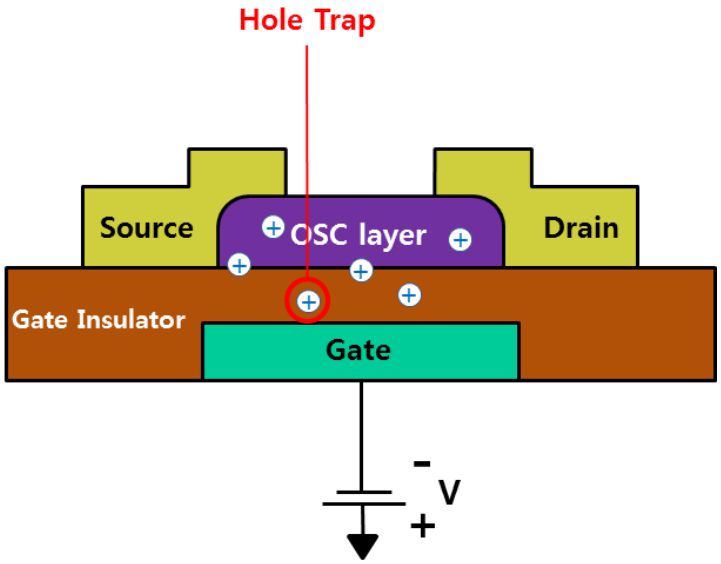

Fig. 2.5. Hole trap formation in an OTFT

while applying negative gate bias stress.

produced in the OTFT device structure. Due to their effect on charge trap formation, surface properties of a gate insulator, which is interfaced with an organic semiconductor layer, significantly influence the instability of the OTFT. There have been many studies on surface properties dependence of gate bias stress effect [9-11]. Among the probable factors possibly influence instability, a lot of works indicate that the diffusion of water molecule in the air into the interface is one of the main

charge trapping sites. For this reason, hydrophobicity of the gate insulator plays an important role in the formation of charge traps since water molecule could be repelled out of the interface in OTFT using hydrophobic gate insulator.

2.3. Aluminum-Assisted CYTOP Surface Hydrophobicity Modification

As mentioned above, though investigating dependence of bias stress on surface properties such as hydrophobicity is important, the previous studies have limits in that the material replacement of the gate insulator is inevitably accompanied by the change of other surface properties as well. Here, we introduce a novel method to tailor hydrophobicity of gate insulator surface without changing other surface properties.

The hydrophobic fluoropolymer, the CYTOP, was used since the hydrophobicity of the CYTOP could be tailored without changing other surface properties. According to the reference on patterning CYTOP [25-26], the

hydrophobicity of CYTOP surface can be varied by thermal treatment through a serial process of the deposition and removal of an aluminum layer on it. The mechanism of aluminum-assisted surface modification method is depicted in Fig.2.6. Owing to the presence of aluminum on the CYTOP surface, the reorientation of functional end-groups of the CYTOP was induced and remained even after the complete elimination of the aluminum layer [25]. To be specific, acid-base interactions occur between acidic aluminol sites on the aluminum thin film and basic carbonyl functional groups on the side of the CYTOP surface. Then, ionic bonding between these functional groups generates reorientation of the end-functional groups of CYTOP surface. It remains even after wet etching process of aluminum thin film. The hydrophobic nature of the surface finally can be restored by applying thermal treatment over 100°C to the CYTOP layer.

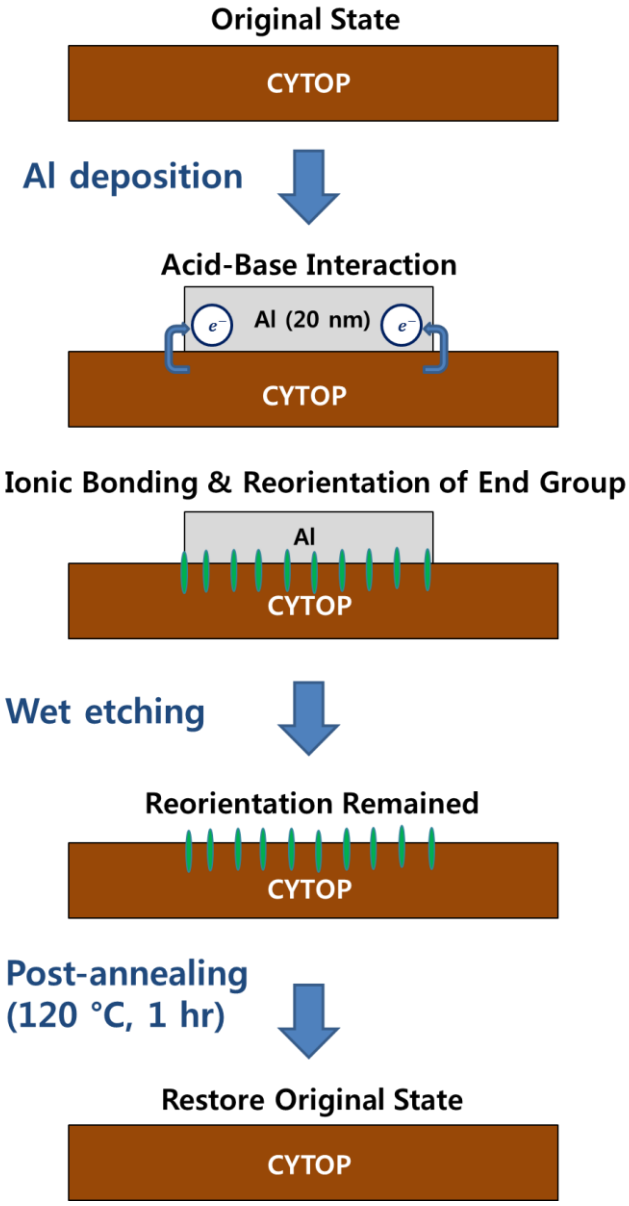

Fig. 2.6. Mechanism of aluminum-assisted

CYTOP surface hydrophobicity modification.

3. Experiments

3.1. Preparation of CYTOP Film with Different Hydrophobicity using Aluminum-Assisted Surface Modification

For verifying our proposed aluminum-assisted surface modification of CYTOP, bare glass substrates were cleaned for tem minutes respectively with acetone, isopropylalcohol, methanol, and deionized water in sequence. A solution of the CYTOP was purchased from Asahi Glass (CTL-809M). It is a solution with 9 wt.% of the CYTOP in perfluorotrialkylamine (CT-solv.180, Asahi Glass Co.). The CYTOP solution was spin-coated onto the glass substrate at the spinning rate of 3000 rpm for 30 s, followed by the subsequent thermal curing at 90 °C for 90 min. A 20 nm-thick aluminum film was thermally deposited onto the CYTOP layer at the rate of 0.1 nm/s under the chamber pressure of 10^{-6} torr. The deposited aluminum film was wet-etched for 3 min at room temperature using an aluminum etchant (Aluminum etchant type D, Transene). The CYTOP layers were then thermally

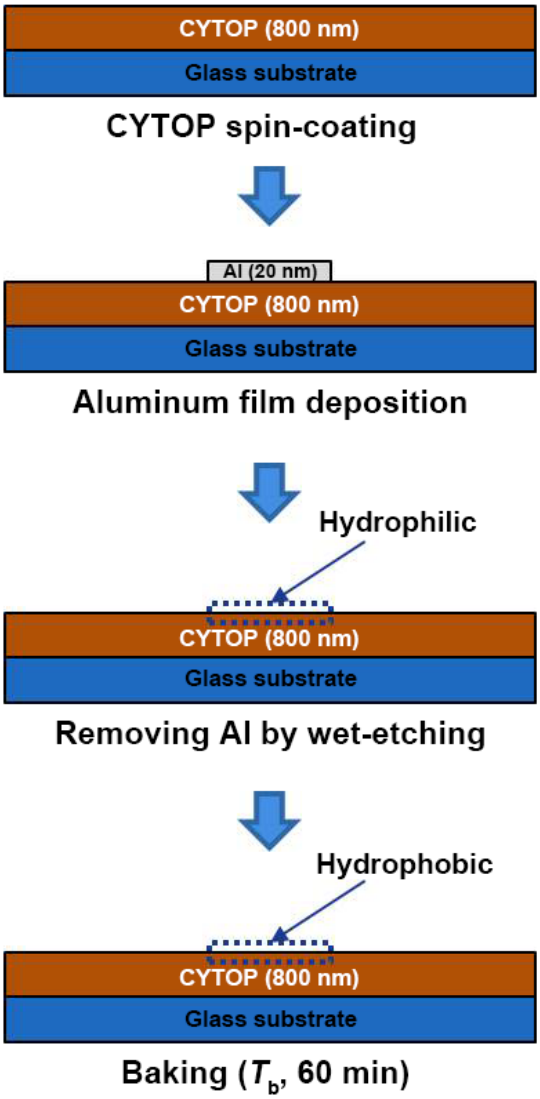

Fig. 3.1. Deposition and removal of an aluminum film on the CYTOP layer together with the baking process.

The baking temperature of the CYTOP layer is denoted by T_b.

treated for 1 hour at four different baking temperatures of T_b = 60, 80, 100, and 120 ℃ to vary the surface hydrophobicity. Fig. 3.1 shows the preparation steps of the CYTOP layer whose hydrophobicity was varied with the baking temperature (T_b).

3.2. Measurement of Contact Angle and Surface Roughness of CYTOP Film

First, we measured the hydrophobicity represented by the contact angle of water droplet on the CYTOP surface. Images of the CYTOP film were first obtained using the optical microscopy, and then the contact angles of water droplet were measured from the microscopic images as shown in the Fig.3.2.

In addition, we measured surface roughness which can also influence gate bias stress effect [9] in order to check whether other surface properties are changed. The topographies of the CYTOP surfaces were observed using the atomic force microscopy (AFM) (XE-100, Park System).

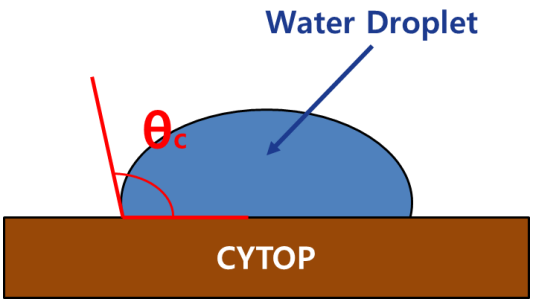

Fig. 3.2. Measurement of the contact angle denoted by θ_c.

3.3. Fabrication of OTFTs with Different Hydrophobicity using Aluminum-Assisted Surface Modification

Using the aluminum-assisted method introduced in the chapter 3.1, we fabricated bottom-gate top-contact OTFT device to verify that the change of hydrophobicity actually influences the device stability. 6,13-bis(triisopropylsilylethynyl)pentacene (TIPS-pentacene) (Sigma Aldrich Co.) was used as an OSC layer. TIPS-pentacene has a structure of pentacene backbone with bulky functional groups at the end of the 6,13 positions of the alkyne and these realize solution-process by enhancement of solubility. Also, the bulky groups improved π-orbital overlap by modifying

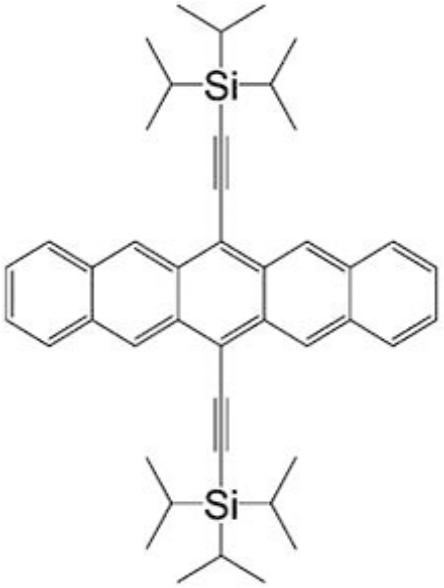

Fig. 3.3. The chemical structure of the TIPS-pentacene.

molecular ordering with face to face interactions [27]. The chemical structure of the TIPS-pentacene is depicted in Fig. 3.3. The fabrication steps of our OTFT are summarized in Fig. 3.4. The CYTOP layer as a gate insulator was spin-coated onto the top of a pre-patterned gate electrode of indium-tin-oxide (ITO) on a glass substrate. The thickness of the gate insulator was about 800 nm. The aluminum film with the pattern of the OSC layer was thermally deposited through a shadow mask onto the CYTOP layer and removed by wet-etching under the same condition

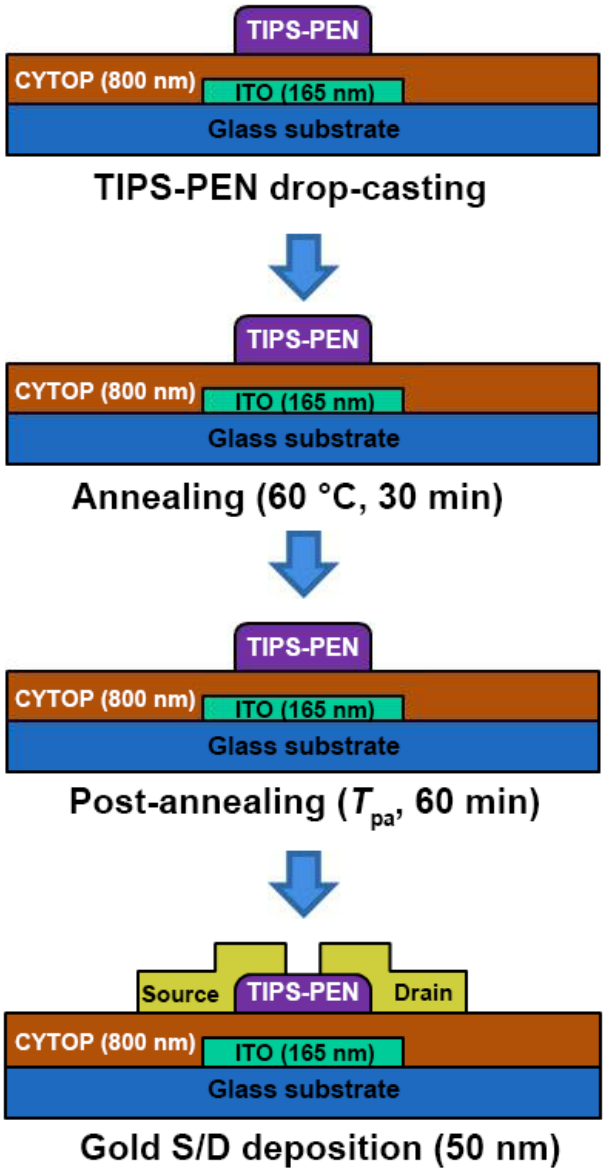

Fig. 3.4. Fabrication and thermal treatment process of our OTFT.

The post-annealing temperature of the OTFT is denoted by T_{pa}.

as described above. The OSC layer was then prepared by drop-casting a solution with1 wt.% of the TIPS-pentacene dissolved in anisole and annealed at 60 ℃ for 30 min. It should be noted that due to the selective wettability [28], the drop-casted TIPS-pentacene was spontaneously confined within the hydrophilic area where the aluminum film was removed as shown in the Fig. 3.5. The fabricated OTFTs were post-annealed for 1 hour at four different temperatures of 60, 80, 100, and 120 ℃ as the case for the CYTOP. The post-annealing temperature (T_{pa}) was chosen to be the same as T_b for self-consistency. Finally, the source and drain electrodes were made of 50 nm-thick gold layers by thermal evaporation through a shadow mask at the

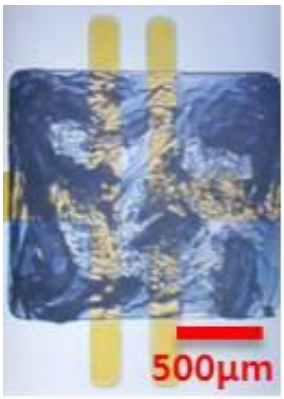

Fig. 3.5. Optical microscopic image of drop-casted TIPS-pentacene confined within hydrophilic area due to hydrophobicity difference.

rate of 0.1 nm/s under the chamber pressure of 10^{-6} torr. The channel width and channel length were 1000 μm and 150 μm, respectively.

3.4. Measurement of OTFT's Electrical Characteristics

The capacitance per unit area, measured using a semiconductor analyzer (4200-SCS, Keithley instruments, Inc.), was 2.36 nF/cm^2. All the measurements of the electrical characteristics were carried out using a semiconductor parameter analyzer (HP 4155A, Agilent Technologies) under ambient conditions.

4. Results and Discussion

4.1. Dependence of Hydrophobicity on Baking Temperature

We first examine the dependence of hydrophobicity represented by the contact angle water droplet on the CYTOP surface treated with different T_b. The contact angle of water droplet represents the degree of how hydrophobic CYTOP surface is. Fig 4.1 (a) corresponds to the microscopic image of untreated CYTOP film, and Fig. 4.1 (b), (c), (d), (e), and (f) correspond to the CYTOP films with thermal treatment of T_b = 25, 60, 80, 100, 120 °C after deposition and removal of aluminum film. As shown in the Fig. 4.1 (a) and (b), the deposition and removal of thin aluminum film transform originally hydrophobic CYTOP into relatively hydrophilic. (contact angle: 110°→77.5°) When the T_b of thermal treatment increased, the hydrophobicity also increased. It is also clearly seen in the Fig 4.2, which represent the measured contact angles as a function of T_b. Although it is already known that deposition and removal of thin aluminum film change CYTOP surface to hydrophilic and the original

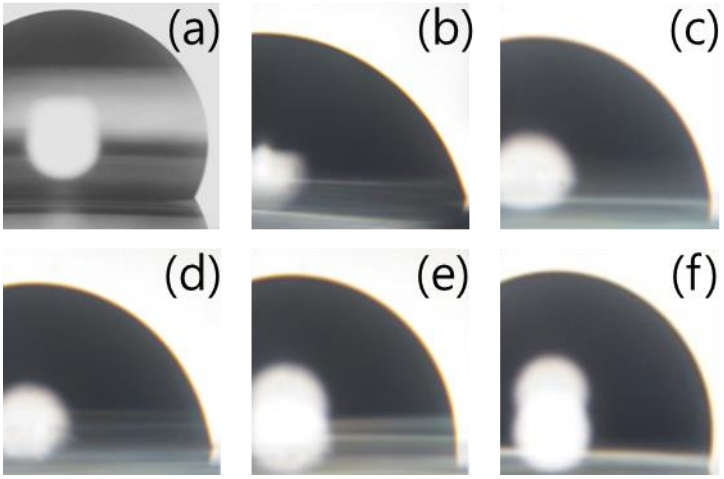

Fig. 4.1. Microscopic images of water droplet on the CYTOP surface. (a) Untreated (b) ~ (f) Thermally treated with baking temperature of 25, 60, 80, 100, and 120 ℃, respectively.

property is recovered by heating [22], we first examined the degree of recovery can be tailored by different T_b. As discussed earlier, this is mainly attributed to the reorientation of functional end-groups. As the T_b increased, the hydrophobic nature of the CYTOP surface became recovered by the thermally-activated relaxation of the reoriented functional end-groups [22-23]. In our case, the contact angle of water on the CYTOP surface increased from 77.5° to 101.8° with increasing T_b from 25℃ to

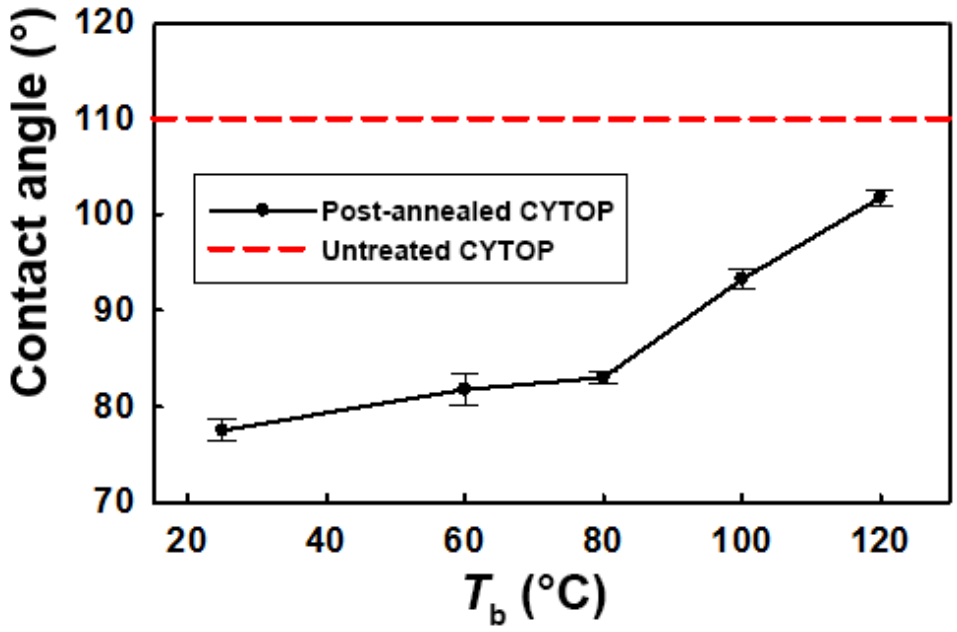

Fig. 4.2. Contact angle of a water droplet on the CYTOP surface as function of the baking temperature T_b. Red dashed line corresponds to the contact angle for the untreated CYTOP.

120℃. In particular, after baked at T_b = 120℃, the contact angle was nearly restored to that for the intrinsic CYTOP surface. This implies that the hydrophobicity of the CYTOP surface can be easily tailored by simply changing T_b through the relaxation of the reoriented functional end-groups of the CYTOP.

4.2. Dependence of Surface Roughness and Morphology on Baking Temperature

Other than hydrophobicity, surface properties such as the surface roughness and the density of hydroxyl group can influence charge trapping in the OTFT device. It is known that threshold voltage shift increased and field-effect mobility of OTFTs decreased as the surface roughness increased. It is because the lattice distortion of active layer may potentially enhance the formation of traps [9]. Also, as the functional group of gate insulator surface can be a potential trap site, high density of hydroxyl group enhanced current hysteresis of OTFTs [10]. Therefore, it should be ensured that the aluminum-assisted surface modification described above involves only the change in the hydrophobicity of the CYTOP surface. Since CYTOP is well known as a hydroxyl-free fluoropolymer, we focused on investigating if the surface roughness and morphology of CYTOP film are changed even after aluminum-assisted surface modification.

Fig. 4.3 (a), (b), and (c) show the AFM images together with the morphological

profiles for the CYTOP surfaces, being untreated, wet-etched, and baked at T_b = 120 ℃, respectively. The corresponding root-mean-square (RMS) values of roughness were 0.408 nm, 0.510 nm, and 0.440 nm, respectively. Note that the absolute values of the RMS roughness for all cases are negligibly small (less than 1 nm), indicating that the surface of CYTOP is highly flat during the aluminum-assisted surface modification. In addition, the deviation for three cases was also small (~ 0.1 nm), and it demonstrates that our modification method did not influence the morphology of the CYTOP film but primarily the hydrophobicity of the CYTOP

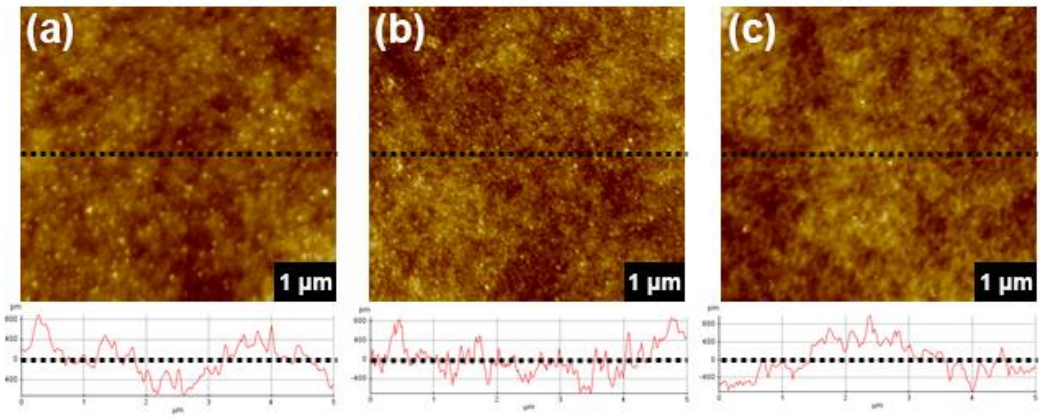

Fig. 4.3. AFM images together with the morphological profiles for the CYTOP surfaces (a) untreated, (b) wet-etched, and (c) baked at T_b = 120 ℃.

surface. The surface roughness was found to be significantly unchanged up to 120 ℃ from room temperature.

4.3. Improvement of Gate Bias Stability in Operating OTFT

Within the framework of only the change of the hydrophobicity of a gate insulator, we now investigate the electrical stability of a solution-processed OTFT against the gate bias stress. For the measurement of the transfer characteristics of the OTFT, the gate voltage (V_G) was swept from 20 V to −50 V at the drain voltage (V_D) of −30 V. For the gate bias stress, V_G = −20 V was applied for 1000 s under the conditions that the source and drain electrodes were grounded for homogenous gate bias condition.

Fig. 4.4 (a), (b), (c), and (d) show the transfer curves of the OTFTs treated thermally under different conditions of no post-annealing, T_{pa} = 80, 100, and 120 ℃, respectively. Blue lines represent the transfer curves of the OTFTs before the gate bias stress, and green lines represent the transfer curves after the gate bias stress. In all cases, typical transfer characteristics of a solution-processed OTFT in a bottom-

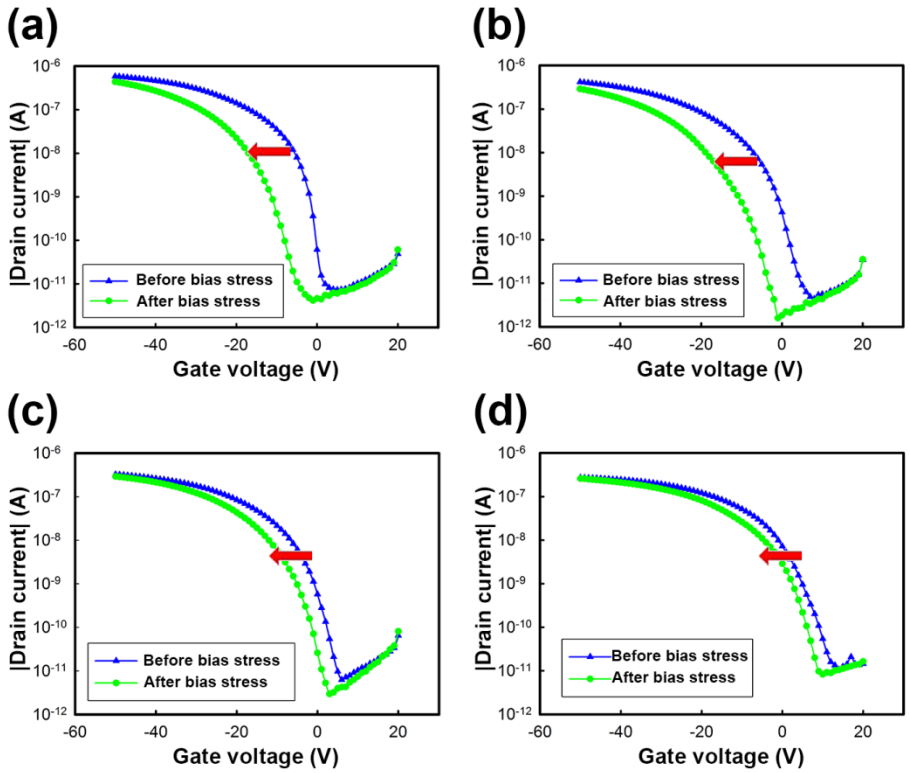

Fig. 4.4. Transfer characteristics of the OTFTs with the CYTOP under different post-annealing conditions of (a) no post-annealing, (b) T_{pa} = 80 ℃, (c) T_{pa} = 100 ℃, and (d) T_{pa} = 120 ℃ for 1 hour before (blue) and after (green) the gate bias stress. Red arrows indicate the shifts of the threshold voltage.

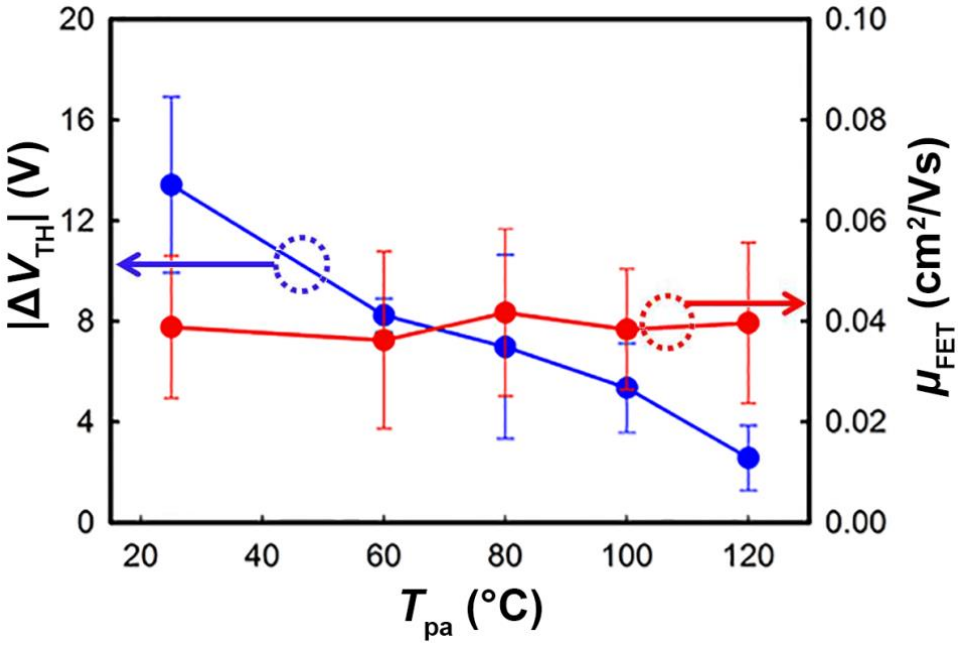

Fig. 4.5. The absolute values of ΔV_{TH} (blue) and μ_{FET} (red) of the OTFTs as a function of T_{pa}.

gate top-contact configuration were observed. It is clearly observed that transfer curves were shifted to negative direction in all cases after gate bias stress due to negative gate bias stress condition. The shift of transfer curve is originated from the formation of the hole traps by diffused water molecules into the interface [12-13]. However, the degree of change in V_{TH} by gate bias stress is different in terms of T_{pa}.

When post-annealing process was not performed, the interface between gate insulator and active layer remains hydrophilic, and therefore fairly large threshold voltage shift after gate bias stress (ΔV_{TH}) is observed (Fig. 4.4(a)). As T_{pa} is increased, however, the interface of gate insulator transforms to hydrophobic, consequently ΔV_{TH} is also reduced. The average values of ΔV_{TH} and μ_{FET} with a function of T_{pa} are summarized in the Fig. 4.5. Especially, when the surface of the gate insulator becomes most hydrophobic (T_{pa} = 120 ℃), the ΔV_{TH} was decreased to the value of −2.56 V from −13.42 V, which is the value for the most hydrophilic surface (No post-annealing). The decreased ΔV_{TH} is attributed to the hydrophobic CYTOP gate insulator, which repels diffusion of water molecules into the interface and therefore suppresses trap formation.

Note that the values of μ_{FET} (0.04±0.01 $cm^2/V{\cdot}s$) and the on/off current ratio (10^5 ~ 10^6) remain consistent regardless of T_{pa}. We could conclude that the post-annealing procedure effected only on the hydrophobicity of the interface. And thus it does not change other parameters of electrical performance but improved electrical stability. Our best OTFT with most hydrophobic surface shows maximum mobility

of 0.063 $cm^2/V \cdot s$, minimum ΔV_{TH} of −1.09 V and negligible hysteresis without any passivation layer under ambient condition. Although cracks were often developed in the TIPS-pentacene layer during thermal annealing at temperatures over 80 ℃ [29], the electrical parameters such as μ_{FET} were not significantly changed under different post-annealing conditions since the TIPS-pentacene layer was pre-annealed before the post-annealing treatment.

5. Conclusion

In summary, we investigated the effect of the hydrophobicity of the gate insulator on the gate bias stress in solution-processed OTFTs. To achieve the electrical stability of the OTFT against the bias stress, the hydrophobicity of the gate insulator was systematically tailored without affecting the surface morphology of the gate insulator using aluminum-assisted surface modification. The average value of ΔV_{TH} by gate bias stress was found to gradually decrease from −13.42 V to −2.56 V as the hydrophobicity of the gate insulator increases. In the best OTFT we fabricated, ΔV_{TH} was measured as small as −1.09 V under the gate bias stress of V_G = −20 V for 1000 s with maximum field-effect mobility of 0.063 cm^2/Vs.

Our aluminum-assisted surface modification approach serves as a useful scheme of tailoring the hydrophobicity of a gate insulator to achieve high electrical stability of the solution-processed OTFT. Also, we introduce a viable method of fabricating and designing the highly stable solution-based OTFTs in the bottom-gate configuration useful for practical circuit application further. In addition, our study is

expected to provide the understanding of physical mechanisms between the gate bias stress effect of the OTFT and hydrophobicity of gate insulator.

Bibliography

[1] H. E. Katz, A. J. Lovinger, J. Johnson, C. Kloc, T. Siegrist, W. Li, Y. Y. Lin, and A. Dodabalapur, *Nature* 404, 478 (2000).

[2] H. Sirringhaus, *Adv. Mater.* 17, 2411 (2005).

[3] S. K. Park, T. N. Jackson, J. E. Anthony, and D. A. Mourey, *Appl. Phys. Lett.* 91, 063514 (2007).

[4] D. Braga and G. Horowitz, *Adv. Mater.* 21, 1473 (2009).

[5] W. H. Lee, H. H. Choi, D. H. Kim, and K. Cho, *Adv. Mater.* 26, 1660 (2014).

[6] M. Matters, D.M. de Leeuw, P.T. Herwig, and A.R. Brown, *Synth. Met*. 102, 998 (1999).

[7] G. W. Hyung, J.-R. Koo, J. H. Seo, J. W. Yang, H. W. Lee, S. W. Pyo, and Y. K. Kim, *J. Nanosci. Nanotechnol.* 11, 4338 (2011).

[8] H. Sirringhaus, *Adv. Mater.* 21, 3859 (2009).

[9] K. Suemori, S. Uemura, M. Yoshida, S. Hoshino, N. Takada, T. Kodzasa, and T. Kamata, *Appl. Phys. Lett.* 93, 033308 (2008).

[10] C. G. Choi and B.-S. Bae, *Electrochem. Solid-State Lett.* 10, H347 (2007).

[11] S. H. Kim, S. Nam, J. Jang, K. Hong, C. Yang, D. S. Chung, C. E. Park, and W. -S. Choi, *J. Appl. Phys.* 105, 104509 (2009).

[12] C. Goldmann, D. J. Gundlach, and B. Batlogg, *Appl. Phys. Lett.* 88, 063501

(2006).

[13] K. P. Pernstich, D. Oberhoff, C. Goldmann, and B. Batlogg, *Appl. Phys. Lett.* 89, 213509 (2006).

[14] H. Klauk, *Chem. Soc. Rev.* 39, 2643 (2010).

[15] T. Umeda, D. Kumaki, and S. Tokito, *Org. Electron.* 9, 545 (2008).

[16] W. L. Kalb, T. Mathis, S. Haas, A. F. Stassen, and B. Batlogg, *Appl. Phys. Lett.* 90, 092104 (2007).

[17] D. K. Hwang, C. Fuentes-Hernandez, J. Kim, W. J. Potscavage, S.-J. Kim, and B. Kippelen, *Adv. Mater.* 23, 1293 (2011).

[18] T. Tsujimura, OLED Display Fundamentals and Applications, *Jon Wiley & Sons* (2012).

[19] I. Kymissis, Organic Field Effect Transistors, *Springers* (2009).

[20] D. Gupta, M. Katiyar, and D. Gupta, *Org. Electron.* 10, 775 (2009).

[21] B. Kumar, B.K. Kaushik, and Y.S. Negi, *Polym. Rev.* 54, 22 (2014).

[22] G. Gu, M.G. Kane, and S. C. Mau, *J. Appl. Phys*. 101, 014504 (2007).

[23] S.H. Han, J.H. Kim, J. Jang, S.M. Cho, M.H. Oh, S.H. Lee, and D.J. Choo, *Appl. Phys. Lett.* 88, 073519 (2006).

[24] B.S. Ong, Y. Wu, P. Liu, and S. Gardner, *J. Am. Chem. Soc*. 126, 3378 (2004).

[25] B. Agnarsson, J. Halldorsson, N. Arnfinnsdottir, S. Ingthorsson, T. Gudjonsson, and K. Leosson, *Microelectron. Eng.* 87, 56 (2010).

[26] P. Degenaar, B. L. Pioufle, L. Griscom, A. Tixier, Y. Akagi, Y. Morita, Y.

Murakami, K. Yokoyama, H. Fujita, and E. Tamiya, *J. Biochem.* 130, 367 (2001).

[27] C. D. Sheraw, T. N. Jackson, D. L. Eaton, and J. E. Anthony, *Adv. Mater.* 15, 2009, (2003).

[28] C.-M. Keum, J.-H. Bae, M.-H. Kim, W. Choi, and S.-D. Lee, *Org. Electron.* 13, 778 (2012).

[29] J.-H. Bae, J. Park, C.-M. Keum, W.-H. Kim, M.-H. Kim, S.-O. Kim, S. K. Kwon, and S.-D. Lee, *Org. Electron.* 11, 784 (2010).

초록

유기 박막 트랜지스터는 낮은 가격, 대면적 공정, 그리고 플렉서블 일렉트로닉스로서의 큰 가능성으로 인하여 많은 관심을 받아왔다. 최근 연구에 따르면, 유기 박막 트랜지스터의 이동도 등 소자의 전기적 성능이 기존에 널리 사용되던 비정질 실리콘 기반 트랜지스터보다 뛰어날 정도로 큰 발전을 이루었다. 그러나 게이트 바이어스 스트레스 효과, 이력현상 등 소자 구동 시 발생하는 불안정성은 유기 박막 트랜지스터의 상용화에 가장 큰 걸림돌이 되었다. 소자의 여러 가지 구성 요소들 중, 게이트 절연막의 표면 거칠기, 표면 하이드록실기 밀도, 또는 소수성 등의 표면 특성이 게이트 절연막과 유기물 층의 계면의 전하 트랩 형성에 영향을 주게 되어 유기물 박막 소자의 안정성을 결정한다. 특히, 게이트 절연막의 소수성은 전하 트랩의 결정적인 요인인 대기 중 물 분자의 유입과 차단에 관여하기 때문에 매우 중요한 역할을 한다. 그러나 소수성에 따른 유기 박막 트랜지스터의 안정성에 대한 연구는 다른 변수들 이외에 소수성만을 조절하기가 어렵다는 이유 때문에 연구가 제한되어 왔다.

본 연구에서는 게이트 절연막의 표면 소수성 유기 박막 트랜지스터의 소자 안정성에 주는 변화와 그 분석에 대하여 알아본다. 소자 안정성을 판단하는 기준으로는 일정한 전압 바이어스를 걸어 주었을 때 문턱전압이 변하는 정도를 사용하였다. 상관관계 분석을 위해, 하나의 게이트 절연막에서 표면 소수성을 다르게 조절한 유기 박막 트랜지스터들을 제작하였다. 본 연구에 사용한 트랜지스터 구조는 바텀 게이트 탑 컨택트 구조이며, 유기물로는 TIPS-Pentacene을, 소수성을 조절할 수 있는 게이트 절연막 물질로는 CYTOP을 사용하였다. 게이트 절연막 표면에 떨어뜨린 물방울의 접촉각으로 표현되는 소수성이 커짐에 따라 문턱전압 변화가 점점 줄어드는 것을 유의미한 결과로서 확인할 수 있었다. 이러한 결과는 계면 소수성이 커짐에 의하여 공기 중 물 분자의 유입이 차단되는 효과에 의한 것으로 예상할 수 있다. 본 연구는 플렉서블 소자 등 다양한 활용 분야에 이용될 수 있는 안정적인 용액 기반 유기 박막 트랜지스터를 위한 이해에 도움을 줄 수 있을 것으로 기대된다.

주요어: Solution-processed organic thin-film transistors, Gate bias stress,

Hydrophobicity, TIPS-pentacene, CYTOP

학번: 2014-22555